



Ultrafast demagnetization in buried Co₈₀Dy₂₀ as fingerprint of hot-electron transport

T. Ferté, N. Bergeard, G. Malinowski, E. Terrier, L. Le Guyader, K. Holldack, M. Hehn, C. Boeglin

► To cite this version:

T. Ferté, N. Bergeard, G. Malinowski, E. Terrier, L. Le Guyader, et al.. Ultrafast demagnetization in buried Co₈₀Dy₂₀ as fingerprint of hot-electron transport. *Journal of Magnetism and Magnetic Materials*, 2019, 485, pp.320-324. 10.1016/j.jmmm.2019.04.068 . hal-02339472

HAL Id: hal-02339472

<https://hal.science/hal-02339472>

Submitted on 22 Oct 2021

HAL is a multi-disciplinary open access archive for the deposit and dissemination of scientific research documents, whether they are published or not. The documents may come from teaching and research institutions in France or abroad, or from public or private research centers.

L'archive ouverte pluridisciplinaire **HAL**, est destinée au dépôt et à la diffusion de documents scientifiques de niveau recherche, publiés ou non, émanant des établissements d'enseignement et de recherche français ou étrangers, des laboratoires publics ou privés.



Distributed under a Creative Commons Attribution - NonCommercial 4.0 International License

Title: Ultrafast demagnetization in buried Co₈₀Dy₂₀ as fingerprint of hot-electron transport

T. Ferté¹, N. Bergeard^{1*}, G. Malinowski², E. Terrier¹, L. Le Guyader³, K. Holldack³, M. Hehn² and C. Boeglin¹

¹ *Université de Strasbourg, CNRS, Institut de Physique et Chimie des Matériaux de Strasbourg, UMR 7504, F-67000 Strasbourg, France.*

² *Institut Jean Lamour, CNRS UMR 7198, Université de Lorraine, 54506 Vandoeuvre-lès-Nancy, France.*

³ *Institut für Methoden und Instrumentierung der Forschung mit Synchrotronstrahlung Helmholtz-Zentrum Berlin für Materialien und Energie GmbH, Albert-Einstein-Str. 15, 12489 Berlin, Germany*

** Corresponding author:*

Mel: nicolas.bergeard@ipcms.unistra.fr

Address: Institut de Physique et de Chimie des Matériaux de Strasbourg (IPCMS)

Campus Cronenbourg 23 rue du Loess BP43 67034 Strasbourg

0. Abstract

The generation of ultrashort hot-electron pulses in metallic heterostructures offers attractive perspectives for the ultrafast spin manipulation on the picosecond time scale. In such approach, the hot-electron pulses are produced by exciting a non-magnetic capping layer with femtosecond infrared laser pulses. These hot-electron pulses propagate towards a buried magnetic layer to trigger ultrafast demagnetization. Lately, it was shown that the demagnetization onset and characteristic demagnetization times are both affected by the transport regime (ballistic or diffusive) of the photo-excited hot-electrons. In this work, we show that the hot-electron pulses produced by photo-exciting a Al(3)/Ta(3)/Cu(60) capping layer undergo a temporal stretching and delays when they go across a [Co(0.1)/Ni(0.6)]_{x5} multilayer. These information were extracted from a study of hot-electron induced demagnetization in CoDy alloys by means of Time-Resolved X-Ray Magnetic Circular Dichroism.

Key words:

Ultrafast demagnetization, Femtosecond laser, Hot-electron pulses, ferrimagnetic alloys

1. Introduction

Since the discovery of sub-picosecond demagnetization in Ni layers by femtosecond infrared (IR) laser pulses [1], the quest towards ultrafast manipulation of spin in magnetic materials has driven many experimental and theoretical investigations [2, 3, 4, 5]. In this context, the All Optical Switching (AOS) of spins on the picosecond time scale induced by a single IR laser pulse appeared as a major technological breakthrough for the data storage technologies [6, 7]. However, this ultrafast reversal has been observed so far for a limited range of materials such as FeCoGd alloys [8] and Co/Gd multilayers [9].

In recent years, sub-picosecond demagnetization induced by hot-electron pulses instead of IR laser pulses was evidenced in a large variety of materials such as ferromagnetic transition metal layers [10, 11], ferromagnetic alloys [12] or multilayers [13] and ferrimagnetic alloys [14]. Subsequently, spin switching induced by a single hot-electron pulse was also demonstrated in FeCoGd alloys [15]. In this alloy, the switching dynamics was shown to be as fast as the reversal by a single IR pulse. In parallel, the ultrafast manipulation of spins in a buried magnetic layer by using spin-polarized (SP) femtosecond hot-electron pulses has triggered intensive researches in the field of “ultrafast spintronics” [16, 17, 18, 19, 20, 21]. The SP femtosecond hot-electron pulses can be generated by exciting a magnetic metal with fs IR laser pulses. This has been theoretically predicted in the superdiffusive spin transport model [22, 23] and evidenced in several experiments [24, 25, 26, 27, 28, 29]. For instance, Alekhin et al. have produced SP hot-electron pulses by photo-exciting a thin Fe capping deposited on a 100 nm thick Au layer to manipulate the magnetization in a buried Fe layer [20]. In such geometry, the metallic capping layer is thicker than the typical IR laser penetration depth to exclude parasitic laser excitations of the buried magnetic layer [30, 12]. Although hot-electron transport in the ballistic regime has been evidenced in thick noble metals layers [31, 32], the actual spin polarization of hot-electrons transferred through tens of nanometers in metals can be questioned. Indeed, Schellekens et al. evidenced a limited spin diffusion length of such hot-electrons in Cu ($\lambda_{Cu} = 13\text{nm}$) [16]. This observation was recently sustained by Iihama et al. [33].

An alternative route to generate and propagate highly SP hot-electron pulses towards a buried magnetic layer consists in generating non polarized hot-electron in a metallic capping layer by using IR laser pulses [5]. A thin magnetic layer is then inserted between the capping metallic

layer and the buried magnetic layer to polarize the hot-electrons via the spin-filtering effect [34].

However, the insertion of a thin metallic layer in the path of the hot-electron pulses could modify the electronic transport properties and subsequently change the magnetization dynamics in the buried magnetic layer. For instance, we have shown that the insertion of a Pt(10) layer between a Pt(3)/Cu(70) capping layer and a CoTb alloys was sufficient to thermalize the photo-excited hot-electrons [14]. We also evidenced that although the demagnetization induced by thermalized hot-electrons (with Pt(10)) is almost as efficient as the demagnetization induced by non-thermalized hot-electrons (without Pt(10)), the characteristic demagnetization times are much longer. We attributed such temporal elongation to the temporal stretching of the thermalized hot-electrons pulse.

In this work, we investigate the changes induced by the insertion of a ferromagnetic [Co(0.1)/Ni(0.6)]_{x5} multilayer on the transport properties of hot-electron pulses. In particular, we are interested in the temporal stretching and delays of the hot-electron pulses. In order to describe these modifications, we have investigated the hot-electron induced demagnetization in a ferrimagnetic Co₈₀Dy₂₀ alloy by means of time-resolved X-ray Magnetic Circular Dichroism (tr-XMCD) [36]. We have considered the characteristic demagnetization times of both Co and Dy sub-lattices to evidence the temporal stretching of the hot-electron pulses and the demagnetization onsets to evidence the temporal delay of the hot-electron pulses as described in our previous work [14]. We show that the insertion of a [Co(0.1)/Ni(0.6)]_{x5} (thickness ~3.5 nm) multilayer results in a huge increase of the characteristic demagnetization time in both the Co 3d and Dy 4f sublattices, as well as a sizable delay of the demagnetization onset. These observations demonstrate that a [Co(0.1)/Ni(0.6)]_{x5} multilayer is capable of efficiently thermalizing the hot-electron pulse before it acts on the CoDy layer.

2. Material and methods

The 18 nm thick Co₈₀Dy₂₀ (label CoDy in the text for commodity) alloys were deposited by DC-magnetron sputtering on SiN membranes and capped with (sample 1) Al(5)/Ta(3), (sample 2) Al(5)/Ta(3)/Cu(60)/[Co(0.1)/Ni(0.6)]_{x5}/Cu(3.5) and (sample 3) Al(5)/Ta(3)/Cu(50)/Pt(9)/ [Co(0.1)/Ni(0.6)]_{x5}/Cu(3.5) multilayers (units in nm). The samples are sketched in figure 1. The choice of the specific materials used as capping layers for samples 2 and 3 (Al(5)/Ta(3)/Cu(X)) ensures negligible direct excitation of CoDy alloys by

IR pump pulses [13, 14] and guarantees at least 15% X-ray transmission at the specific CoL_3 and DyM_5 absorption edges. In sample 2 and 3, the hot-electron pulses are generated by IR absorption in the $\text{Al}(5)/\text{Ta}(3)/\text{Cu}(X)$ capping layers [13]. The $[\text{Co}(0.1)/\text{Ni}(0.6)]_{x5}$ multilayer is the inserted thin magnetic layer. The choice for this material was motivated by its large spin-polarization at the Fermi level [35] which makes it a good candidate for future ultrafast spintronic application. In sample 3, the 9 nm Pt film grown in between the 50nm Cu film and the $[\text{Co}(0.1)/\text{Ni}(0.6)]_{x5}$ multilayers acts as a barrier for the ballistic hot-electrons [14, 17]. **It ensures that the demagnetization is caused by thermalized spin-polarized hot-electrons in sample 3 [14]. By comparing the hot-electron induced demagnetization in sample 2 and 3, we will be able to determine if the demagnetization is caused by non-thermalized or by thermalized spin-polarized hot-electrons in sample 2 [14].** The thin Cu(3.5) layer which is grown in between **the** $[\text{Co}(0.1)/\text{Ni}(0.6)]_{x5}$ multilayers and the buried ferrimagnetic $\text{Co}_{80}\text{Dy}_{20}$ alloy ensures the decoupling between these magnetic layers. We have chosen CoDy alloys instead of the $\text{Co}_{74}\text{Tb}_{26}$ alloys we have previously investigated [14] because they allow investigating the hot-electron induced demagnetization of both the Co 3d “itinerant” and Dy 4f “localized” magnetic moment by tr-XMCD. Indeed, the XMCD amplitude at the Co L_3 edge of the $\text{Co}_{74}\text{Tb}_{26}$ alloys does not match the requirements to perform high quality tr-XMCD at the femtoslicing facility, especially for limited demagnetization amplitudes as those reported in this work (table 1). Furthermore, we have already investigated the direct laser induced demagnetization in CoDy alloys by means of element- and time-resolved XMCD experiments [37]. Therefore, the specificities of the laser and hot-electrons induced ultrafast magnetization dynamics can be easily compared.

The time-resolved XMCD experiments were carried out at the femtoslicing beam line of the BESSY II synchrotron radiation source at the Helmholtz-Zentrum Berlin [36]. We have used the very same configuration for the pump-probe experiments as in a recently published work [14]. The magnetization dynamics have been recorded by monitoring the transmission of circularly polarized X-rays pulses tuned to specific core level absorption edges as a function of a pump-probe delay for two opposite directions of the magnetic field. The photon energy was set to the CoL_3 and the DyM_5 edges using the reflection zone plate monochromator at UE56/1-ZPM. The experimental chamber allowed for mounting two samples, hence, we measured successively samples 1 (direct pumping by IR pulses) and sample 2 or sample 3 (indirect excitation). We determined the temporal and spatial overlap between pump and probe on sample 1 and thus determined accurately the delay induced by the thick capping layers in case of indirect excitation. A 500 μm beam diameter for pump laser was selected in

order to ensure homogeneous pumping over the probed area of the sample (200 μm). The fluences of the laser were set to 7 mJ/cm^2 for sample 1 and 14 mJ/cm^2 for samples 2 and 3. A magnetic field of 0.55 T, sufficient to saturate both the $[\text{Co}(0.1)/\text{Ni}(0.6)]_{\text{x}5}$ multilayer and the CoDy alloys, was applied along the propagation axis of both the IR laser and the X-ray beam during the experiment. Thus, the magnetization directions of both magnetic layers are parallel in our experiment. The temperature of the cryostat was set to 280K to compensate a weak DC-heating for the samples 2 and 3 ($\sim 20\text{K}$) and ensuring an equilibrium temperature of $\sim 300\text{K}$ at negative delays. Thus the experiments were carried out above the temperature of magnetic compensation of the CoDy alloys ($T_{\text{comp}} \sim 220\text{ K}$) [37]. The total amount of Co introduced by the $[\text{Co}(0.1)/\text{Ni}(0.6)]_{\text{x}5}$ multilayers is equivalent to $\sim 0.5\text{ nm}$. This thickness is negligible compared with the Co studied in the buried ferromagnetic $\text{Co}_{80}\text{Dy}_{20}$ alloy ($\sim 14\text{nm}$). Therefore, the contribution of the $[\text{Co}(0.1)/\text{Ni}(0.6)]_{\text{x}5}$ multilayers to the XMCD signal at the Co L_3 edge can be neglected as will be shown.

3. Results and discussions

The transient XMCD recorded for samples 1, 2 and 3 at the Co L_3 and Dy M_5 edges are displayed in figure 2. The experimental data were fitted with two exponential functions (respectively the demagnetization and the magnetization recovery) convoluted by a Gaussian function which accounts for the experimental time resolution (130 fs) [38, 39]. The demagnetization amplitude (q), the demagnetization onset (t_0) and the characteristic demagnetization time (τ) for both Co and Dy sublattices, as well as their error bars extracted from the fits are summarized in table 1. The latter correspond to the standard deviation of experimental data with respect to the fitting function.

Table 1: Parameters extracted from the fit functions for the 3 samples and for both Co and Dy.

	Demagnetization amplitude q (%)	Demagnetization onset t_0 (ps)	Characteristic demagnetization time τ (ps)
Sample 1 Co	51 ± 5	0 ± 0.1	0.16 ± 0.03
Sample 1 Dy	98 ± 5	0 ± 0.1	0.44 ± 0.08
Sample 2 Co	16 ± 3	0.47 ± 0.15	0.33 ± 0.18

Sample 2 Dy	21 ± 3	0.45 ± 0.25	1.95 ± 0.4
Sample 3 Co	9 ± 3	1.1 ± 0.2	0.33 ± 0.2
Sample 3 Dy	19 ± 4	0.9 ± 0.35	2.25 ± 0.6

In sample 1, the demagnetization for both Co and Dy sublattices is driven by direct photon excitations. We observed a demagnetization amplitude $q = 98 \pm 5 \%$ and a characteristic demagnetization times $\tau = 0.44 \pm 0.08$ ps for the Dy 4f sublattice. These values are respectively larger and longer compared to those reported for the Co 3d sublattice ($q = 51 \pm 5 \%$ and $\tau = 0.16 \pm 0.03$ ps). The distinct ultrafast fs-laser induced demagnetization of the TM and the RE sublattices have been reported in various element- and time-resolved XMCD experiments on rare-earth / transition metals alloys [37, 39 - 44]. Even if the discussion of such differences is beyond the scope of this publication, several explanations are proposed in the literature. It may originate from the element-specific dependence of magnetization on temperature in each sublattice [45, 46] as shown by Hofherr et al [47]. It could also arise from heat transfer from the TM sublattice towards the RE sublattice [48]. Gort et al. have demonstrated that the characteristic demagnetization times depend on the electron binding energy [49] while Radu et al. have established a linear relation between τ and the magnetic moments [43]. Anyway, the measurements in sample 1 are used in this study as the references for q , t_0 and τ .

In samples 2 and 3, the demagnetization is caused by the photo-excited hot-electron pulses [5, 13, 14]. Similar to direct IR laser excitation, the hot-electron induced demagnetization of the Co 3d and the Dy 4f sublattices occurs on different time scales in spite of the Co-Dy exchange coupling. By comparing photon- (sample1) and hot-electron- (sample 2 and 3) induced demagnetization, we observe less pronounced demagnetization amplitudes for both the Co and Dy sublattices in the second case. This is obtained in spite of larger laser fluences, and is similar to previously reported results in CoTb alloys [14]. The small demagnetization amplitudes in sample 2 and 3 is partly explained by the large thickness of the $\text{Co}_{80}\text{Dy}_{20}$ alloy (18 nm) compared to the hot-electron penetration depth ($\lambda_{\text{up}}=6.5$ nm for the majority spins and $\lambda_{\text{down}}=1.2$ nm for the minority spins in Co [50]). We also observed delays of the demagnetization onset, and much longer demagnetization times for both Co and Dy sublattices. These observations are of interest here and they are discussed in the following, starting with the characteristic demagnetization times.

Considering the results of our previous work [14], we can state here that the Pt(9) layer in sample 3 is capable of efficiently thermalizing the photo-excited hot-electron pulses. Therefore, the much longer demagnetization times we have observed for both Co (0.33 ps instead of 0.16 ps) and Dy (2.25 ps instead of 0.44 ps) in the case of hot-electron excitation are readily explained. Vodungbo et al. have investigated the hot-electron induced demagnetization in Al(40)/[Co(0.4)/Pd(0.2)]_{x30} multilayer [12]. In their case, the hot-electrons were also thermalized in the Al capping layer before they reach the CoPd multilayer. They have reported a characteristic demagnetization time of 0.43 ps for the Co sublattice instead of 0.16 ps for direct laser induced demagnetization. Their observations are consistent with our measurements at the Co L₃ edge. Interestingly, the characteristic demagnetization times and demagnetization amplitudes measured at Co and Dy edges for samples 2 and 3 are very close, in spite of the additional Pt(9) layer in sample 3. These observations are not compatible with non-thermalized hot-electron induced demagnetization in sample 2 (no Pt) [10, 13, 14]. Indeed, in this case, the characteristic demagnetization times would have been similar to those reported for laser induced demagnetization [14] which is not the case. This means that the demagnetization in sample 2 is most likely induced by thermalized hot-electrons. Therefore, we conclude that the thin [Co(0.1)/Ni(0.6)]_{x5} multilayer is highly efficient to thermalize the hot-electrons which are generated in the Al(5)/Ta(3)/Cu(60) capping layer. This efficiency is probably explained by the hot-electron scattering at the numerous Co/Ni interfaces [51].

The photo-excited hot-electron pulses are not only temporally stretched in the [Co(0.1)/Ni(0.6)]_{x5} multilayers and Pt(9) layers but additionally the group velocity is strongly reduced as suggested by the reported demagnetization onsets for sample 2 (0.47 ± 0.15 ps) and sample 3 (1.1 ± 0.2 ps). These demagnetization onsets are much larger than those previously reported in Pt(3)/Cu(80)/CoPt (~ 0.12 ps) [13]. Such delays are also readily explained by the thermalization of the hot-electrons in the [Co(0.1)/Ni(0.6)]_{x5} multilayers. The values are consistent with those we have reported previously for CoTb alloys with a Pt(10) layer ($\sim 0.35 \pm 0.2$ ps) [14]. **It is worth noticing that the magnetization of the [Co(0.1)/Ni(0.6)]_{x5} multilayer will partly be quenched by the hot-electron pulses [13]. This demagnetization will affect the spin-polarization of the hot-electron pulses [10, 22, 23] and** should occur at $t_0 \sim 0.1$ ps [13]. We do not observe the demagnetization of the [Co(0.1)/Ni(0.6)]_{x5} multilayers because the signal to noise ratio does not allow to resolve the dynamics of such an ultrathin magnetic layer. **Therefore, the longer demagnetization onsets we have reported here** confirm that the transient XMCD signals at the Co L₃ edges measured for sample 2 and 3 (figure 2) are solely defining the ultrafast dynamics in the CoDy alloys.

We show that the $[\text{Co}(0.1)/\text{Ni}(0.6)]_{x5}$ multilayer results in a temporal stretching and a delay of the hot-electron pulses. Therefore, our results suggest that by engineering thin magnetic layers with suitable properties, one can tune the pulse duration of spin-polarized hot-electrons. For instance, recent studies have shown that a longer spin-polarized hot-electron pulse could be more efficient at inducing ultrafast magnetization switching [33, 52]. In this light, our results pave the way to more controlled and efficient magnetization switching.

4. Conclusions

We have reported on the hot-electron induced demagnetization in $\text{Co}_{80}\text{Dy}_{20}$ alloys by element- and time-resolved XMCD. We observed disparate dynamics in terms **of demagnetization times for Co 3d and for Dy 4f sublattices similar to direct laser induced demagnetization.** We have shown that inserting a $[\text{Co}(0.1)/\text{Ni}(0.6)]_{x5}$ multilayer results in a temporal stretching of the photo-excited hot-electron pulses and a reduction of its group velocity. **These tailored SP hot-electron pulses offer prospects for more efficient ultrafast magnetization switching.** This study calls for more systematic experimental and theoretical investigations in order to determine the spin-polarization of the hot-electrons pulses **and how it is affected by the demagnetization of the $[\text{Co}(0.1)/\text{Ni}(0.6)]_{x5}$ multilayer.**

References:

- [1]: Beaurepaire et al. Phys. Rev. Lett., 76, 4250 (1996)
- [2]: Kirilyuk et al. Rev. Mod. Phys., 82, 2731 (2010)
- [3]: Kirilyuk et al. Rep. Prog. Phys. 76, 026501 (2013)
- [4]: Bigot et al. Ann. Phys. 1, 2 (2013)
- [5]: Malinowski et al. Eur. Phys. J. B. 91, 98 (2018)
- [6]: Stanciu et al. Phys. Rev. Lett. 99, 047601 (2007)
- [7]: Ostler et al. Nature Commun. 3, 666 (2012)
- [8]: El Hadri et al. Phys. Rev. B 94, 064412 (2016)
- [9]: Lalieu et al. Phys. Rev. B 96, 220411(R) (2017)
- [10]: Eschenlohr et al. Nature Mater. 12, 332 (2013)
- [11]: Salvatella, Structural Dynamics 3, 055101 (2016)

259 [12]: Vodungbo et al. Scientific Reports 6, 18970 (2016)
 260 [13]: Bergeard et al. Phys. Rev. Lett. 117, 147203 (2016)
 261 [14]: Ferté et al. Phys. Rev. B 96, 144427 (2017)
 262 [15]: Xu et al. Advanced Materials (2017)
 263 [16]: Schellekens et al. Nature Communications 5, 4333 (2014)
 264 [17]: Choi et al. Nature Communications 5, 4334 (2014)
 265 [18]: Choi et al. Nature Physics 11, 576 (2015)
 266 [19]: Razdolski et al. J. of Phys. Condens. Matt. 29, 174002 (2017)
 267 [20]: Alekhin et al. Phys. Rev. Lett. 119, 017202 (2017)
 268 [21]: Baláž et al. J. Phys.: Condens. Matter. 30, 115801 (2018)
 269 [22]: Battiato et al. Phys. Rev. Lett. 105, 027203 (2010)
 270 [23]: Battiato et al. Phys. Rev. B 86, 024404 (2012)
 271 [24]: Malinowski et al. Nature Physics 4, 855 (2008)
 272 [25]: Melnikov et al. Phys. Rev. Lett. 107, 076601 (2011)
 273 [26]: Turgut et al. Phys. Rev. Lett. 110, 197201 (2013)
 274 [27]: Wieczorek et al. Phys. Rev. B 92, 174410 (2015)
 275 [28]: Chen et al. Appl. Phys. Lett. 110, 092407 (2017)
 276 [29]: Shokeen et al. Phys. Rev. Lett. 119, 107203 (2017)
 277 [30]: Khorsand et al. Nature Matter. 13, 101 (2014)
 278 [31]: Brorson et al. Phys. Rev. Lett. 59, 1962 (1987)
 279 [32]: Juhasz et al. Phys. Rev. B 48, 15488 (1993)
 280 [33]: Iihama et al. Advanced Materials. 30, 1804004 (2018)
 281 [34]: Stiles Journal of Appl. Phys. **79**, 5805 (1996)
 282 [35]: Ueda et al. Appl. Phys. Lett. 100, 202407 (2012)
 283 [36]: Holldack et al. J. Synchrotron Rad. 21, 1090 (2014)
 284 [37]: Ferté et al. Phys. Rev. B 96, 134303 (2017)
 285 [38]: Boeglin et al. Nature 465, 458 (2010)
 286 [39]: Bergeard et al. Nature Communications 5, 3466 (2014)
 287 [40]: Radu et al, Nature. 472, 205 (2011)
 288 [41]: Lopez-Flores et al. Phys. Rev. B 87, 214412 (2013)
 289 [42]: Graves et al. Nature Materials. 12, 293 (2013)
 290 [43]: Radu et al. SPIN, 5, 1550004 (2015)
 291 [44]: Higley et al. Rev. of Sci. Instrum. 87, 033110 (2016)
 292 **[45]: Chen et al. Phys. Rev. B 91, 024409 (2015)**

[46]: Donges et al. Phys. Rev. B 96, 024412 (2017)
 [47]: Hofherr et al. Phys. Rev. B 98, 174419 (2018)
 [48]: Mekonnen et al. Phys. Rev. B 87, 180406(R) (2013)
 [49]: Gort et al. Phys. Rev. Lett. 121, 087206 (2018)
 [50] Dijken et al. Phys. Rev. B 66, 094417 (2002)
 [51]: Choi et al. Phys. Rev. B. 89, 064307 (2014)
 [52]: Choi et al. Phys. Rev. B 97, 014410 (2018)

Acknowledgments:

We are indebted for the scientific and technical support given by N. Pontius, Ch. Schüßler-Langeheine and R. Mitzner at the slicing facility at the BESSY II storage ring. The authors are grateful for financial support received from the following agencies: the French “Agence National de la Recherche” via Project No. ANR-11-LABX-0058_NIE and Project EQUIPEX UNION No. ANR-10-EQPX-52, the CNRS-PICS program, the EU Contract Integrated Infrastructure Initiative I3 in FP6 Project No. R II 3CT-2004-50600008. Experiments were carried out on the IJL Project TUBE-Davms equipment funded by FEDER (EU), PIA (Programme Investissement d’Avenir), Region Grand Est, Metropole Grand Nancy, and ICEEL.

The authors have no competing interests to declare

Figures:

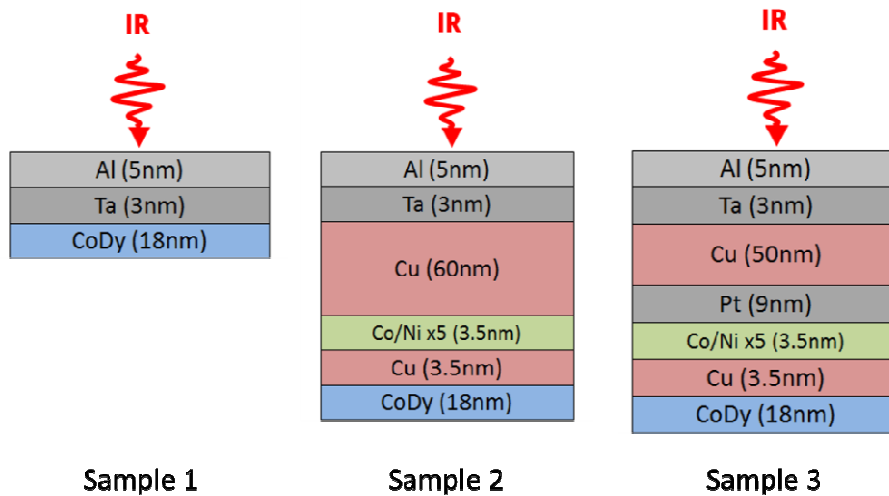


Figure 1: Sketches of the layer structures of the different samples and the geometry of laser excitation (IR, perpendicular to the surface normal).

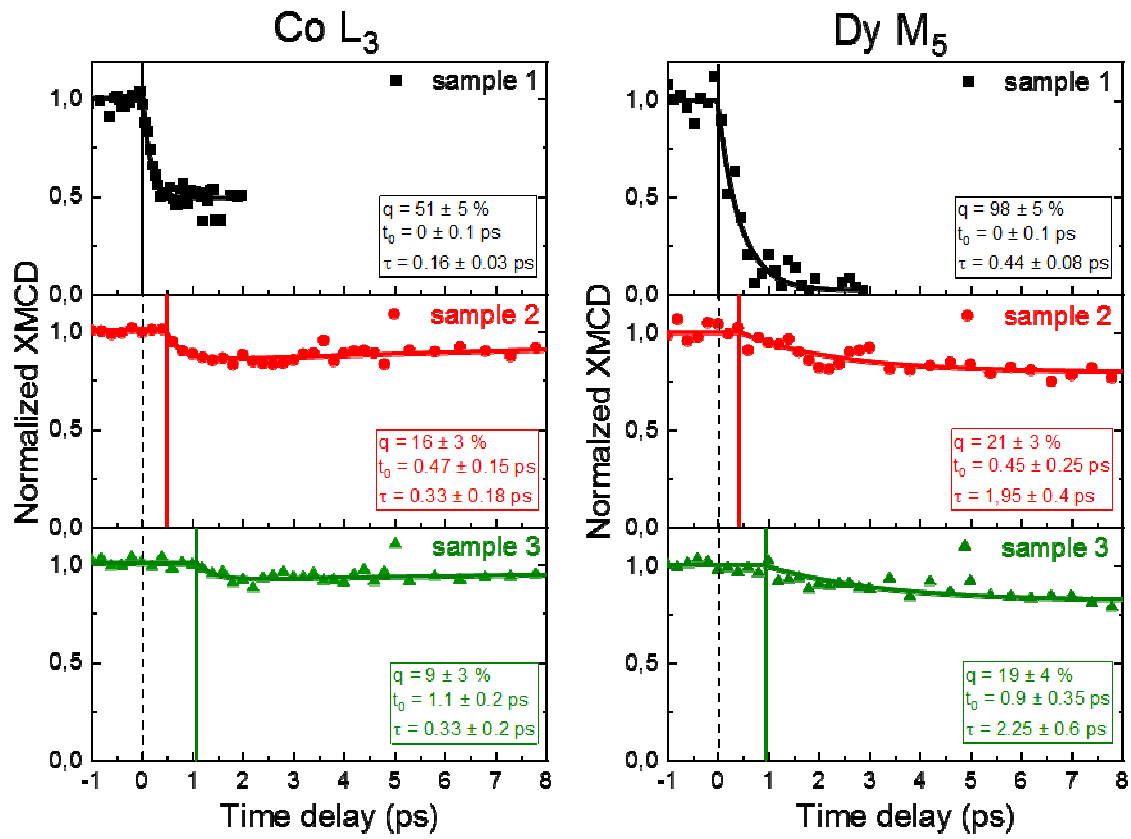


Figure 2: Transient XMCD as a function of the pump-probe delay at the Co L_3 (left column) and Dy M_5 (right column) for sample 1 (black squares), 2 (red circles) and 3 (green triangles) and the corresponding single exponential fits (thick lines). The demagnetization onsets determined from the fits are indicated by the thin vertical lines.